Adaptive waveguide bends with homogeneous, nonmagnetic, and isotropic materials

Tiancheng Han,[1,2] Cheng-Wei Qiu,[2,*] and Xiaohong Tang[1]

[1]*EHF Key Laboratory of Fundamental Science, School of Electronic Engineering, University of Electronic Science and Technology of China, Chengdu, Sichuan 611731, China*

[2]*Department of Electrical and Computer Engineering, National University of Singapore, Kent Ridge, Singapore 119620, Singapore*

**Corresponding author: eleqc@nus.edu.sg*

Received September 22, 2010; revised December 3, 2010; accepted December 4, 2010; posted December 8, 2010 (Doc. ID 135537); published January 11, 2011

We propose a method for adaptive waveguide bends using homogeneous, nonmagnetic, and isotropic materials, which simplifies the parameters of the bends to the utmost extent. The proposed bend has an adaptive and compact shape because of all the flat boundaries. The nonmagnetic property is realized by selecting $OB'/OC = 0.5$. Only two nonmagnetic isotropic dielectrics are needed throughout, and the transmission is not sensitive to nonmagnetic isotropic dielectrics. Results validate and illustrate these functionalities, which make the bend much easier to fabricate and apply, owing to its simple parameters, compact shape, and versatility in connecting different waveguides.

OCIS codes: 230.7370, 160.1190, 130.5296.

Reaching beyond making objects invisible by coordinate transformation [1–4], finite embedded transformation [5] is employed to design beam shifters and splitters. This finite embedded approach is further utilized in conjunction with the design process of waveguide bends [6–10] by use of inhomogeneous and anisotropic materials.

Conventional waveguide bends unfortunately suffer from reflection and also result in the distortion of the guided modes. A few methods have been proposed to obtain waveguide bends of low reflection and minimized mode distortion, such as photonic bends [11], microprism bends [12], and plasmonic bends [13]. Compared to these bends based on photonic crystals and plasmonic guiding modes, the disadvantages of the bends based on finite embedded transformation are obvious, i.e., the use of inhomogeneous, magnetic, and anisotropic metamaterials in the bending part [8], because the involved metamaterials are difficult, if not impossible, to realize in practice.

Therefore, in order to remove the magnetism in the material, simplified parameters are proposed [6]; however, the nonmagnetic material in the bending region is still anisotropic and inhomogeneous along the radial direction [6]. To further remove the inhomogeneity, the inhomogeneous profile of ε_r (along the radial direction) has been discretized into N homogeneous layers [6], i.e., a continuous profile of ε_r replaced with N constant values. To ensure that the discretization is valid, N has to be sufficiently large. However, it should be noted that the material in the bender is still anisotropic in the Cartesian coordinate, and it will thus have N different anisotropic materials in the bender [6]. To further remove the anisotropy in each layer in [6], another discretization is proposed along the azimuth direction [10] by three alternating isotropic dielectrics for an individual layer, resulting in $3N$ different kinds of dielectrics in total. Nevertheless, the material from the identical coordinate transformation [6,10] is inherently inhomogeneous and anisotropic in Cartesian coordinates. To summarize, the transformation optical waveguide bend [6,10] implies that: (i) the bender can connect only two waveguides of equal width and the bender can be only of annular shape; (ii) the material in the bender is inherently inhomogeneous and (or) anisotropic in Cartesian coordinate even after some simplifications; (iii) the discretization along radial direction [6] leads to nonplanar interfaces between layers, while discretization along azimuth direction [10] in each layer leads to titled planar interfaces between dielectrics, which greatly increases the fabrication complexity; and (4) the isotropic structure [10] based on $3N$ (where N denotes the initial number of discretized layers) kinds of dielectrics has physical restrictions on the length of the waveguide (original space) and the bending angle of the bent waveguide (transformed space).

In this connection, a distinguished transformation method is presented here, which demonstrates an interesting advance in the design of waveguide bends based on transformation materials. Compared to the previous waveguide bends [6–10], the bends proposed in this Letter are constructed with homogeneous materials, and they can connect two waveguides of arbitrary widths, while perfect wave tunneling can still be achieved. In addition to the homogeneity, isotropy and nonmagnetism are furthermore introduced into the adaptive bend, which requires only two kinds of isotropic dielectrics for either region throughout. The proposed method can also enable us to shrink the area of the bending region by making the sharp turn obtuse. More interestingly, those shrunken designs are inherently desirable, because they lead us to our utmost aim: homogeneous, nonmagnetic, and isotropic bends. Therefore, our approach provides a much easier but more advantageous recipe for the practical realization of adaptive waveguide bends based on coordinate transformation.

Figure 1 shows the scheme to design waveguide bends by transforming triangles AOB and BOC in virtual space (x, y, z) into AOB' (region I) and $B'OC'$ (region II) in real space (x', y', z'), respectively. It should be noted that the coordinates of points A, B, C, B', and C' are constants and can be expressed as (x_A, y_A), (x_B, y_B), (x_C, y_C), $(x_{B'}, y_{B'})$,

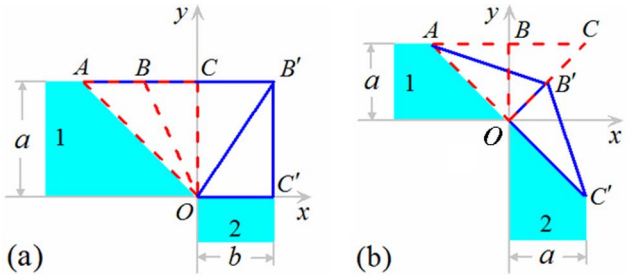

Fig. 1. (Color online) Schematic illustration of coordinate transformation in the design of advanced waveguide bends: (a) bend connecting two waveguides of different widths and (b) bend connecting two waveguides with nonmagnetic materials.

and $(x_{C'}, y_{C'})$, respectively. The transformation equations from the triangle AOB to region I (denoted by the triangle AOB') can be expressed as

$$x' = a_{11}x + b_{11}y + c_{11},$$
$$y' = a_{12}x + b_{12}y + c_{12},$$
$$z' = z, \tag{1}$$

where $[a_{11}, b_{11}, c_{11}]^T = \boldsymbol{Q}_1^{-1}\cdot[x_A, 0, x_{B'}]^T$, $[a_{12}, b_{12}, c_{12}]^T = \boldsymbol{Q}_1^{-1}\cdot[y_A, 0, y_{B'}]^T$, and $\boldsymbol{Q}_1 = [x_A, y_A, 1; 0, 0, 1; x_B, y_B, 1]$.

Based on transformation optics [1,2], the permittivity and permeability of region I can be obtained $\varepsilon_{\mathrm{I}} = \mu_{\mathrm{I}} = \Lambda_1\cdot\Lambda_1^T/\det(\Lambda_1)$, where $\Lambda_1 = [a_{11}, b_{11}, 0; a_{12}, b_{12}, 0; 0, 0, 1]$ and $\det(\Lambda_1) = a_{11}b_{12} - a_{12}b_{11}$.

Region II denoted by triangle $B'OC'$ is transformed from the triangle BOC, and the transformation equations can be expressed as

$$x' = a_{21}x + b_{21}y + c_{21},$$
$$y' = a_{22}x + b_{22}y + c_{22},$$
$$z' = z, \tag{2}$$

where $[a_{21}, b_{21}, c_{21}]^T = \boldsymbol{Q}_2^{-1}\cdot[x_{B'}, 0, x_{C'}]^T$, $[a_{22}, b_{22}, c_{22}]^T = \boldsymbol{Q}_2^{-1}\cdot[y_{B'}, 0, y_{C'}]^T$, and $\boldsymbol{Q}_2 = [x_B, y_B, 1; 0, 0, 1; x_C, y_C, 1]$.

The parameters of region II thus become $\varepsilon_{\mathrm{II}} = \mu_{\mathrm{II}} = \Lambda_2\cdot\Lambda_2^T/\det(\Lambda_2)$, where $\Lambda_2 = [a_{21}, b_{21}, 0; a_{22}, b_{22}, 0; 0, 0, 1]$ and $\det(\Lambda_2) = a_{21}b_{22} - a_{22}b_{21}$.

It can be seen that the constitutive parameters are homogeneous in the two regions of the bender, which greatly enhances the realizability of sharp waveguide bender in practice. Full-wave simulations based on the finite-element method are performed under TM and TE polarization. The waveguide boundaries are assumed to be a perfect electric conductor. First, let us consider a sharp bend designed by the proposed method, which connects two different waveguides. In Fig. 1(a), the widths of the two waveguides are chosen to be $a = 10$ cm and $b = 2$ cm, with their cutoff frequencies at 1.5 GHz and 7.5 GHz, respectively. Figure 2 shows the snapshots of the total electric fields at the working frequency of $f = 10$ GHz, when a TE wave is incident from port 1. If no transformation material is placed in the junction, we can observe that there is nearly no transmission shown in Fig. 2(a). Nevertheless, based on the proposed method, two homogeneous media can be designed and

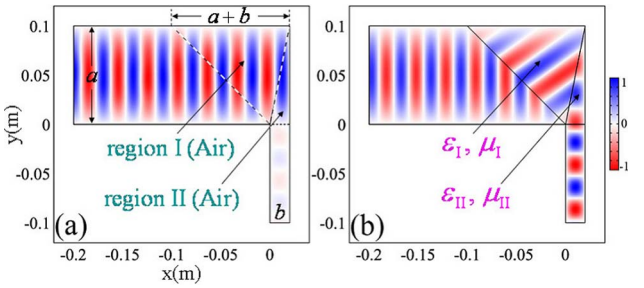

Fig. 2. (Color online) Snapshots of the total electric fields for Fig. 1(a) when $a = 10$ cm and $b = 2$ cm: (a) field distribution without transformation materials in bending region and (b) field distribution with homogeneous transformation materials in the bend.

embedded into respective regions of the bend, as in Fig. 2(b). Then electromagnetic waves can be guided from one waveguide to the other without any reflection. Note that those two homogeneous media in Fig. 2(b) are different, magnetic, and anisotropic.

Then we propose an advanced design in Fig. 3 [based on Fig. 1(b)] to achieve the utmost aim, i.e., a homogeneous, nonmagnetic, and isotropic bend. In addition, this interesting design has a smaller area in the bend and makes the sharp corner obtuse. The symmetry of the tensors ε_{I} and $\varepsilon_{\mathrm{II}}$ ensures that a rotation transformation can map such symmetric tensors into diagonal tensors, from which the effective isotropic media can be derived [14,15]. The permittivity tensor for regions I and II in the bend could be expressed as $\varepsilon_i = \mathrm{diag}[\zeta_i^x, \zeta_i^y, \zeta_i^z]$, where $\zeta_i^x = \left[\varepsilon_i^{xx} + \varepsilon_i^{yy} + \sqrt{(\varepsilon_i^{xx} - \varepsilon_i^{yy})^2 + (2\varepsilon_i^{xy})^2}\right]/2$, $\zeta_i^y = \left[\varepsilon_i^{xx} + \varepsilon_i^{yy} - \sqrt{(\varepsilon_i^{xx} - \varepsilon_i^{yy})^2 + (2\varepsilon_i^{xy})^2}\right]/2$ and $\zeta_i^z = \varepsilon_i^{zz}$ ($i = \mathrm{I}$ or II). Based on the effective media theory, the anisotropic media could be easily realized through alternating layered isotropic media. Because the ideal anisotropic material is homogeneous and identical in both regions, the whole bend now can be composed of only two types of isotropic materials in a planarly layered pattern: medium A and medium B. All isotropic dielectric

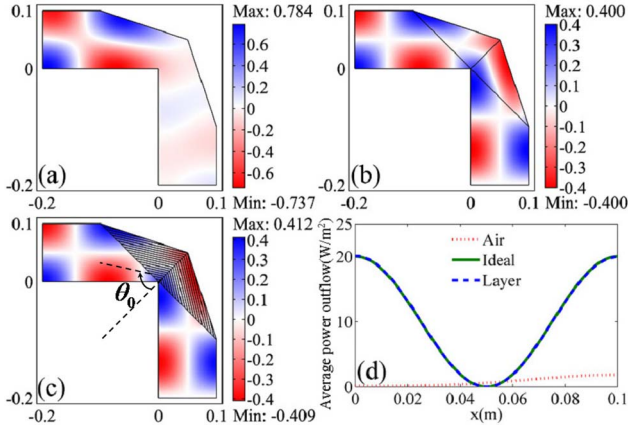

Fig. 3. (Color online) Magnetic field distribution of the bend designed using homogeneous and nonmagnetic materials for $a = 10$ cm, with or without anisotropy: (a) vacuum bend, (b) ideal anisotropic transformation media filled in the bend, (c) layered isotropic dielectrics filled in the bend and $\theta_0 = 58^\circ$, and (d) average power outflow at port 2.

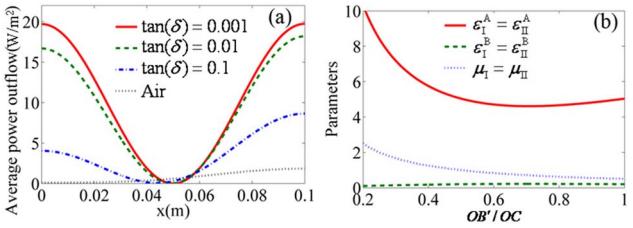

Fig. 4. (Color online) (a) Average power outflow at port 2 when isotropic medium B ε^B is with the loss tangent of 0.001, 0.01, and 0.1 at $OB'/OC = 0.5$ to comply with the nonmagnetic condition. (b) Parameters of two isotropic media versus OB'/OC.

layers are parallel to each other, and the angle between any region I or II layer and the line OB' is $\theta_0 = \frac{\pi}{4} - \frac{1}{2}\tan^{-1}\left(\frac{2\varepsilon_{\mathrm{I}}^{xy}}{\varepsilon_{\mathrm{I}}^{xx}-\varepsilon_{\mathrm{I}}^{yy}}\right)$, where $-\frac{\pi}{2} < \tan^{-1}\left(\frac{2\varepsilon_{\mathrm{I}}^{xy}}{\varepsilon_{\mathrm{I}}^{xx}-\varepsilon_{\mathrm{I}}^{yy}}\right) < \frac{\pi}{2}$. The material parameters of isotropic medium A and medium B are defined as $\varepsilon_i^A = \zeta_i^x + \sqrt{(\zeta_i^x)^2 - \zeta_i^x\zeta_i^y}$ and $\varepsilon_i^B = \zeta_i^x - \sqrt{(\zeta_i^x)^2 - \zeta_i^x\zeta_i^y}$, respectively. The effective isotropic parameters can be found $\varepsilon_{\mathrm{I}}^A = \varepsilon_{\mathrm{II}}^A = 5$, $\varepsilon_{\mathrm{I}}^B = \varepsilon_{\mathrm{II}}^B = 0.2$, and $\mu_{\mathrm{I}} = \mu_{\mathrm{II}} = 1$ when $OB'/OC = 0.5$ to cater to the nonmagnetic requirement.

Figures 3(a) and 3(b) correspond to the nonmagnetic bender with and without transformation media, when a TM wave is incident form port 1 at the working frequency $f = 2$ GHz. Clearly, in Fig. 3(a), strong reflection and severe mode distortion will be present. In Fig. 3(b), EM waves completely pass through the bender with homogeneous, nonmagnetic and ideal anisotropic transformation media. Figure 3(c) presents the magnetic field distribution inside the homogeneous, nonmagnetic, and isotropic bend at $OB'/OC = 0.5$, which is believed to be the most advanced. The anisotropy in Fig. 3(b) has been removed by replacing the identical anisotropic material in regions I and II with two isotropic dielectrics $\varepsilon_{\mathrm{I}}^A = \varepsilon_{\mathrm{II}}^A = 5$, $\varepsilon_{\mathrm{I}}^B = \varepsilon_{\mathrm{II}}^B = 0.2$, and $\mu_{\mathrm{I}} = \mu_{\mathrm{II}} = 1$. In Fig. 3(d), it is clear that the advanced bend is as perfect as the ideal case. More importantly, in each region, the homogeneous, nonmagnetic, and isotropic dielectrics are in planarly layered geometry, and one needs just two kinds of dielectrics for one region, in contrast to the complex configuration and totally $3N$ kinds of different isotropic dielectrics in [10].

Because the dielectric medium B ε^B will have positive permittivity below 1, it is necessary to investigate the loss effect in ε^B. In Fig. 4(a) we plot the average power outflow exiting from port 2 when medium B ε^B has the loss tangent of 0.001, 0.01, and 0.1. It is expected that the average power outflow decreases as the loss increases. An interesting phenomenon is that the power is zero at $x = 0$ m and very low at $x = 0.1$ m for the hollow bend, but the power transmission has been significantly enhanced near those two boundaries when the lossy isotropic dielectrics are filled in the bend. To provide guidelines to the practical implementation, Fig. 4(b) outlines the material parameters as a function of OB'/OC. It reveals that all of ε^A, ε^B, and μ vary slightly when OB'/OC is not quite small, which make such design insensitive to the mismatch between the parameters and the bend shape (OB'/OC). One can also design a 90° bender (i.e., $OB'/OC = 1$); the effective permittivities of the two isotropic dielectrics are identical to the case of $OB'/OC = 0.5$ in Fig. 3(c), but the bender will be magnetic, i.e., $\mu_{\mathrm{I}} = \mu_{\mathrm{II}} = 0.5$ and $\theta_0 = 32^\circ$.

In conclusion, we have proposed an advanced waveguide bending mechanism exploiting homogeneous, nonmagnetic, and isotropic materials, which is more feasible and closer to future realization. In terms of the configuration of isotropic structures, the current model also outperforms the previous designs, because it supports different waveguides and involves much fewer isotropic dielectrics and easier positioning for individual isotropic dielectrics. The full-wave simulation validates the proposed design mechanism, and perfect wave tunneling is demonstrated for the advanced bend with the elimination of reflection and mode distortion. The approach developed here may also find potential applications in optical devices, because multilayered structures can now be fabricated accurately in the nanoscale.

This research was supported by grant R-263-000-574-133 from the National University of Singapore. T. C. Han is working toward his Ph.D. at National University of Singapore.

References

1. U. Leonhardt, Science **312**, 1777 (2006).
2. J. B. Pendry, D. Schurig, and D. R. Smith, Science **312**, 1780 (2006).
3. A. V. Kildishev and V. M. Shalaev, Opt. Lett. **33**, 43 (2008).
4. R. Liu, C. Ji, J. J. Mock, J. Y. Chin, T. J. Cui, and D. R. Smith, Science **323**, 366 (2009).
5. M. Rahm, S. A. Cummer, D. Schurig, J. B. Pendry, and D. R. Smith, Phys. Rev. Lett. **100**, 063903 (2008).
6. W. X. Jiang, T. J. Cui, X. Y. Zhou, X. M. Yang, and Q. Cheng, Phys. Rev. E **78**, 066607 (2008).
7. J. Huangfu, S. Xi, F. Kong, J. Zhang, H. Chen, D. Wang, B.-I. Wu, L. Ran, and J. A. Kong, J. Appl. Phys. **104**, 014502 (2008).
8. D. A. Roberts, M. Rahm, J. B. Pendry, and D. R. Smith, Appl. Phys. Lett. **93**, 251111 (2008).
9. B. Vasic, G. Isic, R. Gajic, and K. Hingerl, Phys. Rev. B **79**, 085103 (2009).
10. X. J. Wu, Z. F. Lin, H. Y. Chen, and C. T. Chan, Appl. Opt. **48**, G101 (2009).
11. A. Mekis, J. C. Chen, I. Kurland, S. Fan, P. R. Villeneuve, and J. D. Joannopoulos, Phys. Rev. Lett. **77**, 3787 (1996).
12. T. Lee and J.-M. Hsu, Appl. Opt. **37**, 3948 (1998).
13. G. Veronis and S. Fan, Appl. Phys. Lett. **87**, 131102 (2005).
14. C. W. Qiu, L. Hu, X. F. Xu, and Y. J. Feng, Phys. Rev. E **79**, 047602 (2009).
15. T. C. Han and C. W. Qiu, Opt. Express **18**, 13038 (2010).